The effects of anisotropy in Jahn–Teller systems: application to the icosahedral $H \otimes (h \oplus g)$ system

2003 J. Phys.: Condens. Matter 15 5697

(http://iopscience.iop.org/0953-8984/15/33/304)

INSTITUTE OF PHYSICS PUBLISHING JOURNAL OF PHYSICS: CONDENSED MATTER

J. Phys.: Condens. Matter **15** (2003) 5697–5714 PII: S0953-8984(03)64120-2

The effects of anisotropy in Jahn–Teller systems: application to the icosahedral $H \otimes (h \oplus g)$ system

J L Dunn, C A Bates, C P Moate[1] and Y M Liu[2]

School of Physics and Astronomy, University of Nottingham, University Park, Nottingham NG7 2RD, UK

E-mail: Janette.Dunn@nottingham.ac.uk and Colin.Bates@nottingham.ac.uk

Received 27 May 2003
Published 8 August 2003
Online at stacks.iop.org/JPhysCM/15/5697

Abstract

Jahn–Teller (JT) coupling between electronic motion and lattice or molecular vibrations results in an adiabatic potential energy surface that contains either wells or troughs of minimum-energy points. When wells are lowest in energy, the system will vibrate about the minimum-energy points. This vibration must be taken into account when describing the quantum mechanical states of the system. In general, the wells will be intrinsically anisotropic. This anisotropy alters the vibrational frequencies and hence the positions of the energy levels, and can be particularly significant when the barriers between wells are shallow. In this paper, we will show how anisotropic states and their energies can be calculated using two unitary transformations. The first locates minima on the adiabatic potential energy surface, and the second accounts for anisotropy in the shape of the minima. The method is developed in a way general enough to allow it to be applied to any linear JT problem. The theory is then applied to the icosahedral $H \otimes (h \oplus g)$ JT system. The results obtained will help the understanding of, for example, the effects of vibronic coupling in positively charged fullerene ions.

1. Introduction

Jahn–Teller (JT) coupling between orbital and vibrational motion is known to be an important feature in a wide range of molecules and crystals. In particular, the electrons in the fullerene molecule C_{60} are strongly coupled to vibrations of the molecular cage. The effects of this coupling can be seen directly in features observed in spectroscopic experiments. Coupling between inter- and intra-molecular vibrational modes is also believed to play an important part

[1] Present address: R205, QinetiQ, Malvern, UK.

[2] Present address: School of Mathematical Sciences, University of Nottingham, University Park, Nottingham NG7 2RD, UK.

0953-8984/03/335697+18$30.00

in various phase transitions seen in fullerene solids, including superconducting transitions in A_3C_{60} fullerides.

A good starting point for studies of JT systems is to analyse the shape of the lowest adiabatic potential energy surface (APES). In many cases, minima (wells) are present. The system will vibrate about the positions of the lowest-energy wells, as well as tunnelling between wells with the same energy (in what is known as the dynamic JT effect). In general, the wells are not isotropic, with the frequency of vibration being different in different directions in coordinate space. In some systems, the anisotropic frequencies differ only slightly from the isotropic ones and anisotropic effects can be neglected for many purposes. However, in other cases the anisotropy is very important. This is particularly true if the JT coupling is such that the barriers between wells are shallow. In other JT systems, linear coupling will result in troughs of minimum energy in the APES rather than distinct wells. However, higher-order couplings will warp the bottom of the trough to again give minima at discrete positions. Such minima are highly anisotropic with the barriers in the directions around the trough being significantly lower than those in directions across the trough. Hence the frequencies of vibration in the directions around the trough are much lower.

The effects of anisotropy are difficult to include in JT models. When anisotropy is neglected, coupling to a vibrational mode of frequency ω in systems with wells in the APES can be modelled in terms of harmonic oscillator-like states with frequency ω. To include anisotropic effects, it is necessary to split the vibrational modes in the region of a minimum into local modes of lower symmetry, and construct appropriate vibronic states from the results. In this paper, we will show how anisotropy can be incorporated in any linear JT system with wells by applying two unitary transformations, one to fix the positions of the wells and one to incorporate anisotropy into the wells.

This paper extends the theory of anisotropy already presented for other cubic [1, 2] and icosahedral [3–6] JT systems, both by giving the result in general terms and in extending the method to overcome limitations with the previous approaches. Anisotropy was introduced into the $T \otimes t$ system using a perturbation approach to include that part of the Hamiltonian usually neglected by the ST method by correcting the wavefunction in a well in the APES to second order [19]. It therefore includes contributions from one- and two-phonon states. The local mode frequencies of vibration within each minimum were therefore also corrected to second order. To obtain exact results, it would be necessary to extrapolate the method to infinite order, as discussed in more detail in [19]. The limitation arises because the perturbation method used did not automatically correct the original frequency of vibration to those of the anisotropic local modes. However, these limitations can be overcome if a scale transformation is introduced. A scale transformation was first introduced by Liu *et al* [1] in a study of the $T \otimes t_2$ JT system. Values for the local mode frequencies can be found by minimizing the energy of states modified by the scale transformation with respect to the local mode frequencies. The values of the local mode frequencies in the strong-coupling limit agreed with those calculated using the well known method of Öpik and Pryce [20]. However, the energies of the minima, and therefore also of the tunnelling states, were found to be higher than those without anisotropy. This is incorrect because the scale transformation is a variational method which should lower the energy. The discrepancy arose because the scale transformation was applied to zeroth-order wavefunctions associated with the wells, even though the energy using these states was calculated to second order. To be consistent, the wavefunction must also be corrected to second order. We will show how this discrepancy may be removed by combining the methods of [19] and [1].

The influence on the local mode frequencies and energies of the tunnelling states will be derived in general terms and discussed in detail. These properties are the important features of

JT systems which allow direct contact to be made between experimental results (such as those from infra-red and Raman spectroscopy) and theory. We will then illustrate the method by applying it to the icosahedral $H \otimes (h \oplus g)$ JT system, discussing in which cases anisotropy can be ignored and in which it is important. The $H \otimes (h \oplus g)$ JT system is of much current interest due to its potential applicability to positively doped fullerene ions. Although it is currently very difficult to manufacture hole-doped fullerene materials, there is some experimental evidence for a strong dynamic JT effect in C_{60}^{+} [7]. Results obtained for these systems may help answer questions such as whether materials containing positively charged ions can be superconducting like their negatively charged counterparts.

The isotropic $H \otimes (h \oplus g)$ JT system and its subsystems $H \otimes h$ and $H \otimes g$ have been extensively studied by a number of groups [8–13], including a calculation of vibronic coupling constants [14]. The current authors studied the $H \otimes h$ subsystem [15] and then the full $H \otimes (g \oplus h)$ system [16, 17], using an analytical, strong-coupling method based around a unitary shift transformation (ST) of the Hamiltonian. The ST procedure effectively displaces the phonon coordinates to the centres of minima on the energy surface and results in states which are automatically vibronic. It was shown that there are minima of either D_{5d} or D_{3d} symmetry on the energy surface (depending on the values of the relevant coupling coefficients) and that, for certain coupling strengths, tunnelling between the D_{3d} minima can lead to a singlet ground state instead of the expected quintet. A physical explanation of the crossover of the ground state of the $H \otimes h$ JT system from an H state to an A state has also been given [18]. These results will be extended to include the effects of anisotropy.

2. The scale transformation

Previous papers [1, 4] have used a scale transformation to introduce anisotropy into problems in which there is coupling to one active vibrational mode. In the case when there is more than one active mode, the ideal situation would be to consider the case where the scale transformation has dimension equal to the sum of the dimensions of all the vibronic modes, which therefore accounts for anisotropic mixing between the different modes Γ. However, the result is very complicated. We will therefore apply separate scale transformations for each mode. The appropriate form of the scale transformation is thus

$$U_{\mathrm{s}} = \prod_{\Gamma} \exp\left(\sum_{\gamma\gamma'} (\Lambda_\Gamma)_{\gamma\gamma'} (b_{\Gamma\gamma} b_{\Gamma\gamma'} - b^{\dagger}_{\Gamma\gamma} b^{\dagger}_{\Gamma\gamma'}) \right) \tag{1}$$

where the labels γ and γ' refer to components of the vibrational mode Γ and the $b^{\dagger}_{\Gamma\gamma}$ and $b_{\Gamma\gamma}$ are phonon creation and annihilation operators. The $(\Lambda_\Gamma)_{\gamma'\gamma}$, which can be viewed as elements of a matrix Λ_Γ, are variational parameters. The transformation can be applied to coordinates $Q_{\Gamma\gamma}$, as given in equation (9) of [1]. This gives

$$U_{\mathrm{s}}^{\dagger} Q_{\Gamma\gamma} U_{\mathrm{s}} = \sum_{\gamma'} \mathrm{e}^{-2\Lambda}_{\gamma'\gamma} Q_{\Gamma\gamma'}, \tag{2}$$

where the $\exp(-2\Lambda)_{\gamma'\gamma}$ are elements of a matrix $\exp(-2\Lambda)$, and where the exponential of a matrix is defined in terms of a power series expansion [21]. Thus it can be seen that the effect of the scale transformation is to introduce a change in the scaling of the original nuclear coordinates. The effect of the scale transformation on this wavefunction can be visualized by transforming the $Q_{\Gamma\gamma}$ *backwards*, i.e. according to the matrix $\exp(2\Lambda)$.

The physical meaning of the scale transformation can be understood by considering the ground state wavefunction of a simple harmonic oscillator in coordinate form.

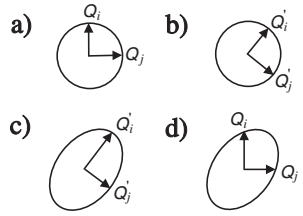

Figure 1. Schematic representation of the effect of the scale transformation on a minimum in a two-dimensional vibrational space. (a) An isotropic minimum is described in terms of normal-mode coordinates Q_i and Q_j. (b) These are then changed to coordinates Q_i' and Q_j' appropriate to the local modes associated with the minimum. (c) The normal modes are scaled to reflect the anisotropy of the minimum. (d) The coordinates are returned to the original normal-mode coordinates Q_i and Q_j.

The wavefunction for γ isotropic oscillators, each of mass μ and frequency ω_Γ, can be written as

$$\Psi_{\mathrm{SHO}}^{\mathrm{iso}} \propto \exp\left(-\frac{\mu\omega_\Gamma}{2\hbar}\sum_\gamma Q_{\Gamma\gamma}^2\right) \tag{3}$$

where the $Q_{\Gamma\gamma}$ are the standard normal-mode coordinates used to describe the JT system in question. An anisotropic oscillator will be composed of vibrations of frequency $\omega_{\Gamma'}$ in directions $Q'_{\Gamma\gamma}$ which, in general, are not the same as the $Q_{\Gamma\gamma}$. The wavefunction must therefore be written in terms of these new local-mode coordinates, which will be different for each minimum in question. The required wavefunction is

$$\Psi_{\mathrm{SHO}}^{\mathrm{anis}} \propto \exp\left(-\frac{\mu}{2\hbar}\sum_\gamma \omega_{\Gamma'} Q'^2_{\Gamma\gamma}\right). \tag{4}$$

The scale transformation must therefore convert $\Psi_{\mathrm{SHO}}^{\mathrm{iso}}$ into $\Psi_{\mathrm{SHO}}^{\mathrm{anis}}$.

Figure 1 illustrates graphically the required transformations for a system with two normal-mode coordinates Q_i and Q_j. The first step is to change from the coordinates Q_i and Q_j (figure 1(a)) to local mode coordinates Q_i' and Q_j' (figure 1(b)). This can be achieved using a unitary matrix S composed of eigenvectors of the so-called curvature matrix [5] appropriate to that minimum. The curvature eigenvectors must then be scaled to generate an anisotropic minimum (figure 1(c)) by multiplying them by another matrix T involving the anisotropic frequencies. Finally, the first transformation must be undone and the original group theoretical coordinates regained by multiplying by $S^\dagger$ (figure 1(d)).

Mathematically it is found that, in the general case, an appropriate form for the matrix T is a diagonal matrix $[\sqrt{\lambda_{\Gamma'}}]$ in which the diagonal elements are $\sqrt{\lambda_{\Gamma'}}$, where $\lambda_{\Gamma'}$ is the ratio of the frequency of the local mode of symmetry γ' to the original frequency, $\lambda_{\Gamma'} = \omega_{\Gamma'}/\omega_\Gamma$. The required form for $\exp(2\Lambda)$ is thus

$$\mathrm{e}^{2\Lambda} = S^\dagger \cdot [\sqrt{\lambda_{\Gamma'}}] \cdot S. \tag{5}$$

This definition of the matrix $\exp(2\Lambda)$ is realized if the matrix Λ takes the form

$$\Lambda = \tfrac{1}{4} S^\dagger \cdot [\ln(\lambda_{\Gamma'})] \cdot S \tag{6}$$

where $[\ln(\lambda_{\Gamma'})]$ is a diagonal matrix with diagonal elements $\ln(\lambda_{\Gamma'})$. It should be noted that although the S matrices appearing in the scale transformation will be different for each minimum in the APES, the local mode frequencies $\lambda_{\Gamma'}$ are the same for all minima of the same symmetry.

3. Perturbation theory

3.1. The scale transformation of the Hamiltonian

In this section, we will describe the effect of applying both the shift and scale transformations to a general linear JT Hamiltonian, allowing for coupling to vibronic modes of more than one symmetry. The general JT Hamiltonian is $\mathcal{H} = \mathcal{H}_{\rm osc} + \mathcal{H}_{\rm int}$ where

$$\begin{aligned} \mathcal{H}_{\rm osc} &= \frac{1}{2}\sum_{\Gamma\gamma}\left[\frac{P_{\Gamma\gamma}^2}{\mu} + \mu\omega_\Gamma^2 Q_{\Gamma\gamma}^2\right] \\ \mathcal{H}_{\rm int} &= \sum_{\Gamma\gamma} V_\Gamma \hat{L}_{\Gamma\gamma} Q_{\Gamma\gamma} \end{aligned} \tag{7}$$

and $P_{\Gamma\gamma}$ is the momentum conjugate to $Q_{\Gamma\gamma}$, the V_Γ are vibronic coupling coefficients and the $\hat{L}_{\Gamma\gamma}$ are operators characterizing the vibronic interaction. On applying the shift transformation $U_{\rm d} = \exp(-\sum_{\Gamma\gamma}\alpha_{\Gamma\gamma}P_{\Gamma\gamma})$ and scale transformation (1) to $\mathcal{H}$, we obtain the transformed Hamiltonian $\tilde{\mathcal{H}} = \tilde{\mathcal{H}}_1 + \tilde{\mathcal{H}}_2 + \tilde{\mathcal{H}}_3$, where

$$\begin{aligned} \tilde{\mathcal{H}}_1 &= \sum_{\Gamma\gamma}\hbar\omega_\Gamma\left(\frac{\alpha'^2_{\Gamma\gamma}}{4} + (\sinh^2 2\Lambda_\Gamma)_{\gamma\gamma}\right) - \frac{1}{\sqrt{2}}\sum_{\Gamma\gamma} k_\Gamma \hat{L}_{\Gamma\gamma}\alpha'_{\Gamma\gamma} \\ \tilde{\mathcal{H}}_2 &= \sum_{\Gamma}\sum_{\gamma\gamma'}\left\{\left(-\frac{1}{\sqrt{2}}k_\Gamma\hat{L}_{\Gamma\gamma} + \frac{\hbar\omega_\Gamma}{2}\alpha'_{\Gamma\gamma}\right)[(b_{\Gamma\gamma'} + b^\dagger_{\Gamma\gamma'})\mathrm{e}^{-2\Lambda_\Gamma}_{\gamma'\gamma}]\right\} \\ \tilde{\mathcal{H}}_3 &= \sum_{\Gamma\gamma}\hbar\omega_\Gamma(b^\dagger_{\Gamma\gamma}b_{\Gamma\gamma} + \tfrac{1}{2}) \end{aligned} \tag{8}$$

and where the coefficients are

$$k_\Gamma = V_\Gamma\sqrt{\frac{\hbar}{\mu\omega_\Gamma}}, \qquad \alpha'_{\Gamma\gamma} = \alpha_{\Gamma\gamma}\sqrt{2\mu\omega_\Gamma\hbar}. \tag{9}$$

$\tilde{\mathcal{H}}'_1$ does not depend on the phonon operators, $\tilde{\mathcal{H}}'_2$ does contain phonon operators, and $\tilde{\mathcal{H}}'_3$ is an oscillator Hamiltonian. Terms quadratic in the phonon operators have been ignored in $\tilde{\mathcal{H}}'_2$ [1].

The eigenstates of $\tilde{\mathcal{H}}'_1$ in the infinite-coupling limit are denoted by X_i, with $i = 0$ for the ground state. The corresponding energies of these states are E_i^X. Multiplying by the eigenstates of the oscillator Hamiltonian $\tilde{\mathcal{H}}'_3$ gives the unperturbed basis set; the ground state will be denoted by $|X_i; 0\rangle$, the state with one phonon excitation of symmetry $\Gamma\gamma$ will be denoted $|X_i; 1_{\Gamma\gamma}\rangle$ etc. The effects of anisotropy may be found by incorporating $\tilde{\mathcal{H}}'_2$, up to second order in perturbation theory, within these states. The energy of a minimum X is therefore given by

$$E_X = E_0^X + \langle X_0; 0|\tilde{\mathcal{H}}'_2|X_0; 0\rangle + \sum_{i\neq 0,\Gamma\gamma}\frac{|\langle X_i; 1_{\Gamma\gamma}|\tilde{\mathcal{H}}'_2|X_0; 0\rangle|^2}{E_0^X - E_i^X - \hbar\omega_\Gamma}. \tag{10}$$

By minimizing this expression with respect to the variational parameters $\lambda_{\Gamma'}$, the values of these parameters may be fixed. Thus the local mode frequencies are found as a function of the coupling strength. This is an improvement over the method of Öpik and Pryce [20], which only gives values for these frequencies in the infinite-coupling limit.

3.2. The anisotropic corrections

Having separated the transformed Hamiltonian in the way described in the previous section, the corrections to the wavefunctions can be found by standard perturbation theory. From the form

of the perturbing Hamiltonian $\tilde{\mathcal{H}}'_2$, the ground phonon state is only coupled to singly excited phonon states in first order and to doubly excited (or two-) phonon states in second order. However, there is a problem using non-degenerate perturbation theory for some of these two-phonon states. Those two-phonon states which have an energy just above the ground orbital state ($i = 0$) become degenerate with the ground state in the strong-coupling limit and they would therefore cause infinities to appear in the resulting equations (compare with equation (3.25) of [19]). Thus not all of the second-order terms are necessarily included in the wavefunction using non-degenerate perturbation theory. Rather than including an incomplete set of states, we approximate by ignoring all the two-phonon states in this paper. Fortunately, the two-phonon terms do not actually affect the energy of the minima to second order. This arises because, as they occur in the second-order correction to the wavefunction, their only possible contribution to the energy would be via the matrix element $\tilde{\mathcal{H}}'_1$, between themselves and the zeroth-order (zero-phonon) wavefunction. (Note that all other matrix elements would be higher than second order in perturbation theory.) As $\tilde{\mathcal{H}}'_1$ contains no phonon operators, this matrix element is in fact zero. The only effect of these terms is, therefore, on the overlap and the matrix elements of the Hamiltonian between *different* minima. Therefore, in the infinite-coupling limit, the wavefunction will remain correct, although some accuracy will be lost in the tunnelling regime.

In the sum over one-phonon states, it might be thought that a similar problem would arise if one-phonon states just above the ground orbital state ($i = 0$) were included. In fact, this is not the case as the matrix element of $\tilde{\mathcal{H}}'_2$ is automatically zero for these states. Thus the corrected wavefunction for the ground minimum X in the transformed space takes the form

$$\psi_X = |X_0; 0\rangle + \sum_{i\neq 0,\Gamma\gamma} \mathcal{Z}_1^X(i,\Gamma\gamma)|X_i; 1_{\Gamma\gamma}\rangle + \mathcal{Z}_2^X|X_0; 0\rangle. \tag{11}$$

The coefficients $\mathcal{Z}_1^X(i,\Gamma\gamma)$ and $\mathcal{Z}_2^X$ are found by evaluating the appropriate matrix elements of the perturbing Hamiltonian, with the results

$$\begin{aligned} \mathcal{Z}_1^X(i,\Gamma\gamma) &= \sum_{\gamma'} \frac{\left(-\frac{1}{\sqrt{2}}k_\Gamma\langle X_0|\hat{L}_{\Gamma\gamma'}|X_i\rangle + \frac{1}{2}\delta_{i0}\hbar\omega_\Gamma\alpha'_{\Gamma\gamma'}\right)\mathrm{e}^{-2\Lambda_\Gamma}_{\gamma\gamma'}}{E_0^X - E_i^X - \hbar\omega_\Gamma} \\ \mathcal{Z}_2^X &= -\tfrac{1}{2}\sum_{i,\Gamma\gamma}(\mathcal{Z}_1^X(i,\Gamma\gamma))^2. \end{aligned} \tag{12}$$

It is useful to look at the way in which these coefficients change as the coupling strength increases. As $k_\Gamma \to \infty$ and considering only one vibrational mode for simplicity, we find that the first-order coefficient $\mathcal{Z}_1^X(i,\Gamma\gamma)$ is proportional to $1/k_\Gamma$, while the second-order coefficient is proportional to $1/k_\Gamma^2$. Thus, in strong coupling, the wavefunction is dominated by the zeroth-order term $|X_0; 0\rangle$, confirming that the original separation of the transformed Hamiltonian into $\tilde{\mathcal{H}}'_1 + \tilde{\mathcal{H}}'_3$ and $\tilde{\mathcal{H}}'_2$ is valid.

In the untransformed space, the anisotropic wavefunction is $\Psi_X = U_{\mathrm{d}}^X U_{\mathrm{s}}^X \psi_X$, where U_{d}^X and U_{s}^X are the shift and scale transformations respectively for well X. The next sections will show how this wavefunction may be used to find the new energy of a minimum and the overlap and Hamiltonian matrix elements between different minima. We note that the energy of a minimum, corrected to second order, may be found either by evaluating matrix elements of the wavefunction Ψ_X or by using equation (10). (Both calculations give the same result, which provides a useful check on the calculations.) For a general well X, the corrected ground state energy is $E_X = E_X^{(0)} + E_X^{(2)}$, where

$$E_X^{(0)} = -\frac{1}{2}\sum_{\Gamma\gamma}\frac{k_\Gamma}{\sqrt{2}}\langle X_0|\hat{L}_{\Gamma\gamma}|X_0\rangle\alpha'_{\Gamma\gamma} + \sum_{\Gamma\gamma}\hbar\omega_\Gamma\left(\frac{1}{2} + (\sinh^2 2\Lambda_\Gamma)_{\gamma\gamma}\right) \tag{13}$$

is the zeroth-order energy and

$$E_X^{(2)} = \frac{1}{2}\sum_{\Gamma}\sum_{i,\gamma,\gamma'}\frac{k_\Gamma^2\langle X_0|\hat{L}_{\Gamma\gamma}|X_i\rangle\langle X_0|\hat{L}_{\Gamma\gamma'}|X_i\rangle \mathrm{e}^{-4\Lambda_\Gamma}_{\gamma\gamma'}}{E_0 - E_i - \hbar\omega_\Gamma} \tag{14}$$

is the second-order correction. First-order corrections are zero.

When determining the well energy from the matrix elements of Ψ_X, the unitary transformations on each side of the Hamiltonian $\hat{\mathcal{H}}$ are the same. Thus the Hamiltonian may be transformed into $\tilde{\mathcal{H}}_1'$, $\tilde{\mathcal{H}}_2'$ and $\tilde{\mathcal{H}}_3'$ and their matrix elements easily evaluated. However, this will not be the case for overlaps and matrix elements between two different minima, A and B, which are therefore harder to evaluate. In order to calculate the overlap, it is necessary to calculate terms such as $\langle\Psi_A|\Psi_B\rangle$. Unfortunately, such expressions cannot be evaluated using the method of second quantization used for isotropic cases [15–17]. In order to proceed, it is therefore advantageous to switch to semi-classical coordinate space and perform the overlap calculation using integral calculus directly.

3.2.1. The semi-classical form for the anisotropic wavefunction. To zeroth order, the general form for an anisotropic ground state vibronic wavefunction localized in a minimum X is

$$\Psi_X^{(0)} \propto U_{\mathrm{d}}^X U_{\mathrm{s}}^X \prod_{\Gamma}\exp\left(-\frac{\mu\omega_\Gamma}{2\hbar}\sum_{\gamma} Q_{\Gamma\gamma}^2\right)|X_0\rangle. \tag{15}$$

In the last section, it was shown that the effect of U_{s}^X is to introduce a coordinate change in the $Q_{\Gamma\gamma}$ via the matrix $\mathrm{e}_A^{2\Lambda}$ (equation (2)). Similarly, the effect of U_{d}^X is to displace the coordinates $Q_{\Gamma\gamma}$ to the centre of the minimum X. Thus the above wavefunction may be simplified to

$$\Psi_X^{(0)} = \prod_{\Gamma} N_\Gamma \exp\left(-\frac{\mu\omega_\Gamma}{2\hbar}(\vec{Q}_\Gamma + \vec{\alpha}_\Gamma^X\hbar)^\dagger\cdot(\mathrm{e}_X^{4\Lambda_\Gamma})\cdot(\vec{Q}_\Gamma + \vec{\alpha}_\Gamma^X\hbar)\right)|X_0\rangle \tag{16}$$

where the vector $\vec{\alpha}_\Gamma^X$ has components $\alpha_{\Gamma\gamma}^X$. The normalization constants N_Γ for each mode Γ can be evaluated using the form of the matrix $\mathrm{e}_X^{2\Lambda}$ given in equation (5), with the result

$$N_\Gamma = \left(\frac{\mu\omega_\Gamma}{\pi\hbar}\right)^{n_\Gamma/4}\sqrt{\det(\mathrm{e}_X^{2\Lambda_\Gamma})} \equiv \prod_{\Gamma'=1}^{n_\Gamma}\left(\frac{\mu\omega_{\Gamma'}}{\pi\hbar}\right)^{1/4} \tag{17}$$

where n_Γ is the dimensionality of the vibronic mode Γ.

Although second quantized notation cannot be used to evaluate the overlap itself, it can be used to write one-phonon states etc in terms of the semi-classical zero-phonon state obtained above. Thus a state with a single phonon excitation γ in well X may be written as

$$U_{\mathrm{d}}^X U_{\mathrm{s}}^X|1_{\Gamma\gamma}\rangle = -\sqrt{\frac{2\mu\omega_\Gamma}{\hbar}}[(\vec{Q}_\Gamma + \vec{\alpha}_\Gamma^X\hbar)^\dagger\cdot\mathrm{e}_X^{2\Lambda_\Gamma}]_\gamma U_{\mathrm{d}}^X U_{\mathrm{s}}^X|0\rangle \tag{18}$$

where the subscript γ to the square bracket indicates the γth component of the matrix product. Other excited phonon states may also be generated by this mechanism.

3.2.2. Derivation of the zeroth order anisotropic overlap. As the excited states may be expressed in terms of the ground phonon state, the overlap between them will always involve the overlap between two different zeroth-order well states $\Psi_A^{(0)}$ and $\Psi_B^{(0)}$. The latter overlap is given by the integral of $\Psi_A^{(0)*}\Psi_B^{(0)}$ over all $\vec{Q}$, which, with some simplifications and using the identity

$$\int_{-\infty}^{\infty}\exp[-(\vec{Q}^\dagger\cdot M\cdot\vec{Q} - \vec{V}^\dagger\cdot\vec{Q})]\,\mathrm{d}\vec{Q} = \exp\left(\frac{1}{4}\vec{V}^\dagger\cdot M^{-1}\cdot\vec{V}\right)\sqrt{\frac{\pi^n}{\det(M)}} \tag{19}$$

gives

$$S_{AB}^{(0)} = \langle A|B\rangle \prod_{\Gamma} \sqrt{\frac{2^n \det \mathrm{e}_A^{4\Lambda_\Gamma}}{\det W_\Gamma}} \exp\left(\frac{1}{4}\vec{x}_\Gamma^{\dagger} \cdot W_\Gamma^{-1} \cdot \vec{x}_\Gamma\right)$$
$$\times \exp(-\tfrac{1}{4}(\vec{\alpha}_\Gamma'^{A\dagger} \cdot \mathrm{e}_A^{4\Lambda_\Gamma} \cdot \vec{\alpha}_\Gamma'^{A} + \vec{\alpha}_\Gamma'^{B\dagger} \cdot \mathrm{e}_B^{4\Lambda_\Gamma} \cdot \vec{\alpha}_\Gamma'^{B})) \tag{20}$$

where the vector $\vec{x}_\Gamma$ and the matrix W_Γ are defined by

$$\begin{aligned} \vec{x}_\Gamma &= -[\vec{\alpha}_\Gamma'^{A\dagger} \cdot \mathrm{e}_A^{4\Lambda_\Gamma} + \vec{\alpha}_\Gamma'^{B\dagger} \cdot \mathrm{e}_B^{4\Lambda_\Gamma}] \\ W_\Gamma &= \mathrm{e}_A^{4\Lambda_\Gamma} + \mathrm{e}_B^{4\Lambda_\Gamma}. \end{aligned} \tag{21}$$

The factor involving the square root is not present in the isotropic overlap. The physical significance of this term lies in the fact that two anisotropic minima will have an orientation relative to each other. Thus, even if the centres of the two anisotropic minima coincide (in which case the exponential decay term is equal to one) the total phonon overlap need not be unity.

First- and second-order corrections to the overlap involve the overlap of one-phonon states with the ground state. These may be calculated in a similar manner to that given above.

3.3. Anisotropic overlap and matrix elements

The total overlap can now be evaluated. In order to calculate the parts involving the excited states, the identity (19) must be differentiated with respect to the vector $\vec{V}$. The total overlap can then be expressed in the form

$$S_{AB} = S_{AB}^{(0)} \mathcal{F}_{AB} \tag{22}$$

with $S_{AB}^{(0)}$ as found above and

$$\mathcal{F}_{AB} = (1 + \mathcal{F}_{AB}^{(1)} + \mathcal{F}_{AB}^{(2)}). \tag{23}$$

The first-order term in this expression is given by

$$\mathcal{F}_{AB}^{(1)} = -\sum_{i\neq 0,\Gamma\gamma} \mathcal{Z}_1^A(i,\Gamma\gamma)\frac{\langle A_i|B_0\rangle}{\langle A_0|B_0\rangle}[\vec{v}_\Gamma^A \cdot \mathrm{e}_A^{2\Lambda_\Gamma}]_\gamma - \sum_{i\neq 0,\Gamma\gamma} \mathcal{Z}_1^B(i,\Gamma\gamma)\frac{\langle A_0|B_i\rangle}{\langle A_0|B_0\rangle}[\vec{v}_\Gamma^B \cdot \mathrm{e}_B^{2\Lambda_\Gamma}]_\gamma \tag{24}$$

and the second-order term is

$$\mathcal{F}_{AB}^{(2)} = \sum_{i\neq 0}\sum_{j\neq 0}\sum_{\Gamma\gamma}\sum_{\Gamma'\gamma'} \mathcal{Z}_1^A(i,\Gamma\gamma)\mathcal{Z}_1^B(j,\Gamma'\gamma')\frac{\langle A_i|B_j\rangle}{\langle A_0|B_0\rangle} g_{\Gamma\Gamma'\gamma\gamma'}^{AB} \tag{25}$$

where

$$\begin{aligned} \vec{v}_\Gamma^X &= \vec{x}_\Gamma^{\dagger} \cdot W_\Gamma^{-1} + \vec{\alpha}_\Gamma'^{X} \\ g_{\Gamma\Gamma'\gamma\gamma'}^{XY} &= 2\delta_{\Gamma\Gamma'}(\mathrm{e}_X^{2\Lambda_\Gamma} \cdot W_\Gamma^{-1} \cdot \mathrm{e}_Y^{2\Lambda_\Gamma})_{\gamma\gamma'} + [\vec{v}_\Gamma^X \cdot \mathrm{e}_X^{2\Lambda_\Gamma}]_\gamma [\vec{v}_\Gamma^Y \cdot \mathrm{e}_Y^{2\Lambda_{\Gamma'}}]_{\gamma'}. \end{aligned} \tag{26}$$

In the isotropic limit, all the $\lambda_{\Gamma'}$ are equal to unity as found by direct substitution so that $S_{AB}^{(0)}$ reduces back to the isotropic overlap. Similarly, the perturbation corrections reduce back to those given in earlier work by Dunn [22]. This provides a useful check on these expressions.

The matrix elements of the Hamiltonian may be derived using similar techniques, using identity (19) by differentiating with respect to the vector $\vec{V}$. The zeroth-order matrix element of the oscillator Hamiltonian is then found to be

$$(\mathcal{H}_{\mathrm{osc}})_{AB}^{(0)} = S_{AB}^{(0)} \sum_{\Gamma} \frac{\hbar\omega_\Gamma}{2}\{\mathrm{tr}(W_\Gamma^{-1} - \mathrm{e}_B^{4\Lambda_\Gamma} \cdot W_\Gamma^{-1} \cdot \mathrm{e}_B^{4\Lambda_\Gamma} + \mathrm{e}_B^{4\Lambda_\Gamma})$$
$$+ \tfrac{1}{2}(|\vec{x}_\Gamma^{\dagger} \cdot W_\Gamma^{-1}|^2 - |\vec{v}_\Gamma^B \cdot \mathrm{e}_B^{4\Lambda_\Gamma}|^2)\}. \tag{27}$$

In order to calculate the matrix element of the total oscillator Hamiltonian, it is again simpler to write the excited phonon states in terms of the zeroth-order states. The resulting integrals may then be evaluated in the same manner as those for $(\hat{\mathcal{H}}_{\rm osc})^{(0)}_{AB}$. After much algebra, the final form for the matrix element of the oscillator Hamiltonian is

$$(\mathcal{H}_{\rm osc})_{AB} = (\mathcal{H}_{\rm osc})^{(0)}_{AB}\mathcal{F}_{AB} - S^{(0)}_{AB}(\mathcal{G}^{(1)}_{AB} + \mathcal{G}^{(2)}_{AB}) \tag{28}$$

where

$$\mathcal{G}^{(1)}_{AB} = -\sum_{i\neq 0,\Gamma\gamma} \mathcal{Z}^A_1(i,\Gamma\gamma)\frac{\langle A_i|B_0\rangle}{\langle A_0|B_0\rangle}\hbar\omega_\Gamma h^{BA}_{\Gamma\gamma} - \sum_{i\neq 0,\Gamma\gamma} \mathcal{Z}^B_1(i,\Gamma\gamma)\frac{\langle A_0|B_i\rangle}{\langle A_0|B_0\rangle}\hbar\omega_\Gamma h^{AB}_{\Gamma\gamma}$$

$$\begin{aligned}\mathcal{G}^{(2)}_{AB} = \sum_{i\neq 0}\sum_{j\neq 0}\sum_{\Gamma\gamma}\sum_{\Gamma'\gamma'} \mathcal{Z}^A_1(i,\Gamma\gamma)\mathcal{Z}^B_1(j,\Gamma'\gamma')\frac{\langle A_i|B_j\rangle}{\langle A_0|B_0\rangle}(\hbar\omega_{\Gamma'}[\vec{v}^A_\Gamma\cdot \mathrm{e}^{2\Lambda_\Gamma}_A]_\gamma[h^{BB}_{\Gamma'} - \vec{v}^B_{\Gamma'}\cdot \mathrm{e}^{6\Lambda_{\Gamma'}}_B]_{\gamma'} \\ + \hbar\omega_\Gamma[\vec{v}^B_{\Gamma'}\cdot \mathrm{e}^{2\Lambda_{\Gamma'}}_B]_{\gamma'}h^{BA}_{\Gamma\gamma} + 2\delta_{\Gamma\Gamma'}\hbar\omega_\Gamma[m^{ABB}_\Gamma - (\mathrm{e}^{2\Lambda_\Gamma}_A\cdot W^{-1}_\Gamma\cdot \mathrm{e}^{6\Lambda_\Gamma}_B)]_{\gamma\gamma'})\end{aligned} \tag{29}$$

are first- and second-order corrections respectively and

$$\begin{aligned}h^{XY}_{\Gamma\gamma} &= [(\vec{v}^X_\Gamma\cdot \mathrm{e}^{8\Lambda_\Gamma}_X - \vec{x}^\dagger_\Gamma\cdot W^{-1}_\Gamma)\cdot W^{-1}_\Gamma\cdot \mathrm{e}^{2\Lambda_\Gamma}_Y]_\gamma \\ m^{XYZ}_{\Gamma\gamma\gamma'} &= [\mathrm{e}^{2\Lambda_\Gamma}_X\cdot W^{-1}_\Gamma\cdot(\mathrm{e}^{8\Lambda_\Gamma}_Y - I)\cdot W^{-1}_\Gamma\cdot \mathrm{e}^{2\Lambda_\Gamma}_Z]_{\gamma\gamma'}.\end{aligned} \tag{30}$$

The zeroth-order matrix element of the anisotropic interaction is

$$(\mathcal{H}_{\rm int})^{(0)}_{AB} = S^{(0)}_{AB}\sum_{\Gamma\gamma}\frac{k_\Gamma}{\sqrt{2}}[\vec{x}^\dagger_\Gamma\cdot W^{-1}_\Gamma]_\gamma\frac{\langle A_0|\hat{L}_{\Gamma\gamma}|B_0\rangle}{\langle A_0|B_0\rangle}. \tag{31}$$

In a similar manner, the first-order correction is found to be

$$\begin{aligned}(\mathcal{H}_{\rm int})^{(1)}_{AB} = -S^{(0)}_{AB}\sum_{i\neq 0,\Gamma'\gamma'}\Bigg(&\mathcal{Z}^A_1(i,\Gamma'\gamma')\sum_{\Gamma\gamma}\frac{k_\Gamma}{\sqrt{2}}\frac{\langle A_i|\hat{L}_{\Gamma\gamma}|B_0\rangle}{\langle A_0|B_0\rangle}P^A_{\Gamma\gamma\gamma'} \\ &+ \mathcal{Z}^B_1(i,\Gamma'\gamma')\sum_{\Gamma\gamma}\frac{k_\Gamma}{\sqrt{2}}\frac{\langle A_0|\hat{L}_{\Gamma\gamma}|B_i\rangle}{\langle A_0|B_0\rangle}P^B_{\Gamma\gamma\gamma'}\Bigg)\end{aligned} \tag{32}$$

where

$$P^X_{\Gamma\gamma\gamma'} = \{[\vec{x}^\dagger_\Gamma\cdot W^{-1}_\Gamma]_\gamma[\vec{v}^X_{\Gamma'}\cdot \mathrm{e}^{2\Lambda_{\Gamma'}}_X]_{\gamma'} + 2\delta_{\Gamma\Gamma'}(W^{-1}_\Gamma\cdot \mathrm{e}^{2\Lambda_\Gamma}_X)_{\gamma\gamma'}\}, \tag{33}$$

while the second-order correction is

$$\begin{aligned}(\mathcal{H}_{\rm int})^{(2)}_{AB} = (\mathcal{H}_{\rm int})^{(0)}_{AB}(\mathcal{Z}^A_2 + \mathcal{Z}^B_2) + S^{(0)}_{AB}\sum_{i\neq 0}\sum_{j\neq 0}\sum_{\Gamma'\gamma'}\sum_{\Gamma''\gamma''}\mathcal{Z}^A_1(i,\Gamma'\gamma')\mathcal{Z}^B_1(j,\Gamma''\gamma'') \\ \times\sum_{\Gamma\gamma}\frac{k_\Gamma}{\sqrt{2}}\frac{\langle A_i|\hat{L}_{\Gamma\gamma}|B_j\rangle}{\langle A_0|B_0\rangle}\{[\vec{x}^\dagger_\Gamma\cdot W^{-1}_\Gamma]_\gamma g^{AB}_{\Gamma'\Gamma''\gamma'\gamma''} \\ + 2\delta_{\Gamma\Gamma'}(W^{-1}_\Gamma\cdot \mathrm{e}^{2\Lambda_\Gamma}_A)_{\gamma\gamma'}[\vec{v}^B_{\Gamma''}\cdot \mathrm{e}^{2\Lambda_{\Gamma''}}_B]_{\gamma''} + 2\delta_{\Gamma\Gamma'}(W^{-1}_\Gamma\cdot \mathrm{e}^{2\Lambda_\Gamma}_B)_{\gamma\gamma''}[\vec{v}^A_{\Gamma'}\cdot \mathrm{e}^{2\Lambda_{\Gamma'}}_A]_{\gamma'}\}.\end{aligned} \tag{34}$$

The formulae given above show how the frequencies of vibration around minima in the lowest APES can be determined for any JT system taking anisotropy into account, and how the results can be used to determine wavefunctions and energies of anisotropic vibronic states. We will now illustrate how the formulae can be used by applying them to the icosahedral $H \otimes (h \oplus g)$ JT system. We will also give a physical discussion of the results obtained.

4. Application to the $H \otimes (h \oplus g)$ problem

4.1. Anisotropy in the D_{3d} minima

In order to apply the scale transformation to the basic Hamiltonian, the form of the matrix Λ specific to the D_{3d} minima must be obtained. We should first note that the condition for the D_{3d} minima to be deep is

$$V_{h_b}^2 \ll \frac{5}{9}\left(V_{h_a}^2 + \frac{\omega_h^2}{\omega_g^2}V_g^2\right) \tag{35}$$

so that the coupling constant V_{h_b} appearing in the Hamiltonian (equation (3) of [16], with V_{h_b} replacing V_2) may be safely neglected in $\tilde{\mathcal{H}}_2$.

From group theory, it is known that when the g and h representations of I_h are restricted to the subgroup D_{3d} they split according to

$$g \to a_1 \oplus a_2 \oplus e \qquad h \to a_1 \oplus 2e$$

so that the appropriate form for Λ_g involves $\{\lambda_{g,a}, \lambda_{g,a'}, \lambda_{g,e}, \lambda_{g,e}\}$, while Λ_{h_a} involves $\{\lambda_{h_a,a}, \lambda_{h_a,e}, \lambda_{h_a,e}, \lambda_{h_a,e'}, \lambda_{h_a,e'}\}$. $S \equiv S_k^{D_{3d}}$ is a unitary matrix which reduces the icosahedral h modes into local modes of the above symmetries. Equivalently, it produces a change in the coordinates from the original $(\Gamma\gamma)$ to coordinates which lie along the curvature eigenvectors of the anisotropic kth minimum. In order to find these latter matrices, the curvature matrix for the energy surface at the point of the D_{3d} minimum in question must be calculated. This is straightforward using the method of Öpik and Pryce [20]; the results are given in the appendix.

The first step in applying the scale transformation is the evaluation of the local mode frequencies, $\lambda_{\Gamma'}$. This involves calculating the energy of any one of the D_{3d} minima corrected to second order in perturbation theory, using the perturbing Hamiltonian $\tilde{\mathcal{H}}_2'$ with terms involving V_{h_b} neglected. The result is

$$\begin{aligned} H_{aa}^{D_{3d}} = &-\frac{2}{9}\frac{k_{h_a}^2}{\hbar\omega_h} - \frac{2}{9}\frac{k_g^2}{\hbar\omega_g} + \frac{\hbar\omega_h}{2}\left(\frac{\lambda_{h_a,a}}{2} + \frac{1}{2\lambda_{h_a,a}} + \lambda_{h_a,e} + \frac{1}{\lambda_{h_a,e}} + \lambda_{h_a,e'} + \frac{1}{\lambda_{h_a,e'}}\right) \\ &+ \frac{\hbar\omega_g}{2}\left(\frac{\lambda_{g,a}}{2} + \frac{1}{2\lambda_{g,a}} + \frac{\lambda_{g,a'}}{2} + \frac{1}{2\lambda_{g,a'}} + \lambda_{g,e} + \frac{1}{\lambda_{g,e}}\right) \\ &- \frac{\hbar\omega_h}{2}\frac{k_{h_a}'^2}{\lambda_{h_a,e'}f_{ha,e'}} - \frac{9\hbar\omega_h}{2}\frac{k_{h_a}'^2}{\lambda_{h_a,e}f_{ha,e}} - 5\hbar\omega_g\frac{k_g'^2}{\lambda_{g,e}f_{g,e}} \end{aligned} \tag{36}$$

where

$$\begin{aligned} f_{ha,e} &= 14k_{h_a}'^2 + 5k_g'^2\omega_g/\omega_h + 18 \\ f_{ha,e'} &= 6k_{h_a}'^2 + 15k_g'^2\omega_g/\omega_h + 18 \\ f_{g,e} &= 15k_g'^2 + 6k_{h_a}'^2\omega_h/\omega_g + 18. \end{aligned} \tag{37}$$

Minimization with respect to the $\lambda_{\Gamma'}$ parameters then generates the local mode frequencies

$$\begin{aligned} \lambda_{h_a,a} &= \lambda_{g,a} = \lambda_{g,a'} = 1 \\ \lambda_{h_a,e} &= \sqrt{1 - 9k_{h_a}'^2/f_{ha,e}} \\ \lambda_{h_a,e'} &= \sqrt{1 - k_{h_a}'^2/f_{ha,e'}} \\ \lambda_{g,e} &= \sqrt{1 - 10k_g'^2/f_{g,e}}. \end{aligned} \tag{38}$$

It can be seen that the effect of anisotropy on $\lambda_{h_a,e}$ and $\lambda_{g,e}$ can be quite significant. When coupling to the h_a mode is strong and the g mode is weak, the anisotropic frequency $\omega_{ha,e}$ is

reduced to $\sqrt{5/14} \approx 0.59$ of its isotropic value, and when the coupling to g is strong but that to h_a is weak, the frequency $\omega_{g,e}$ is reduced by a factor $\sqrt{1/3} \approx 0.58$. These frequency changes will be significant in, for example, spectroscopic experiments probing the vibrational states. On the other hand, $\lambda_{h_a,e'}$ is close to unity for all coupling strengths. Therefore, anisotropic changes in this frequency will have little effect on the tunnelling energies. We will thus take this frequency to equal unity in the subsequent calculations.

The energies of the H, A and G tunnelling states have been shown previously [15–17] to be given by the expressions

$$\begin{aligned} E_H^{\mathrm{D_{3d}}} &= \frac{\mathcal{H}_{aa}^{\mathrm{D_{3d}}} - 2\mathcal{H}_{ab}^{\mathrm{D_{3d}}} + \mathcal{H}_{ae}^{\mathrm{D_{3d}}}}{1 - 2S_{ab}^{\mathrm{D_{3d}}} + S_{ae}^{\mathrm{D_{3d}}}} \\ E_A^{\mathrm{D_{3d}}} &= \frac{\mathcal{H}_{aa}^{\mathrm{D_{3d}}} + 6\mathcal{H}_{ab}^{\mathrm{D_{3d}}} + 3\mathcal{H}_{ae}^{\mathrm{D_{3d}}}}{1 + 6S_{ab}^{\mathrm{D_{3d}}} + 3S_{ae}^{\mathrm{D_{3d}}}} \\ E_G^{\mathrm{D_{3d}}} &= \frac{\mathcal{H}_{aa}^{\mathrm{D_{3d}}} + \mathcal{H}_{ab}^{\mathrm{D_{3d}}} - 2\mathcal{H}_{ae}^{\mathrm{D_{3d}}}}{1 + S_{ab}^{\mathrm{D_{3d}}} - 2S_{ae}^{\mathrm{D_{3d}}}}. \end{aligned} \tag{39}$$

Thus there are two possible overlaps between different wells, and similarly also two possible off-diagonal Hamiltonian matrix elements. These may be calculated using the general expressions derived above. Unfortunately, the results are too complicated to give here as analytical expressions.

The results for the corrected overlap and Hamiltonian matrix elements cannot be substituted directly into the expressions for the tunnelling energies given in equation (39) because the overlaps and matrix elements have been corrected to second order, but when they are substituted into equation (39) they will contain some higher-order contributions. Therefore, the contributions to the tunnelling energies must be separated into zeroth-, first- and second-order parts, with higher-order terms being neglected. The resulting tunnelling splittings $E_A^{\mathrm{D_{3d}}}$–$E_H^{\mathrm{D_{3d}}}$ and $E_G^{\mathrm{D_{3d}}}$–$E_H^{\mathrm{D_{3d}}}$ are too complicated to show as 3D graphs due to the behaviour at weak coupling when the limiting values depend upon the way the limiting point is reached. In order to see the effects of anisotropy on the tunnelling splittings more clearly, results for the pure $H \otimes h$ system were plotted as a function of the coupling strength in [6]. It was found that the calculated values of the tunnelling splitting including anisotropy were much closer to numerical results obtained using a Lanczos diagonalization procedure than values calculated without anisotropy. Figure 2 shows the tunnelling splittings for the $H \otimes g$ JT system. Results including the perturbation correction but excluding the scale transformation are also shown. It is clear that, while the perturbation correction decreases the tunnelling splitting, the scale transformation then increases it again (though not by as much). The effect of both the scale transformation and perturbation correction is to lower the energy of the states involved. However, the perturbation correction has a larger effect on the ground state than the excited state for the scale transformation. This is seen as an increase in the difference in energy between the two states.

4.2. Anisotropy in the D_{5d} minima

The condition that the $\mathrm{D_{5d}}$ wells are absolute minima is the reverse of the inequality in equation (35). Therefore, the problem is effectively reduced from the $H \otimes (h \oplus g)$ JT system to the simpler $H \otimes h$ JT system involving only h-type phonon operators in the scale transformation. Thus the matrix Λ for the $\mathrm{D_{5d}}$ minima is a square 5×5 matrix. From group theory, the h representation of the icosahedral group splits according to $h \rightarrow a_1 \oplus e_1 \oplus e_2$ when

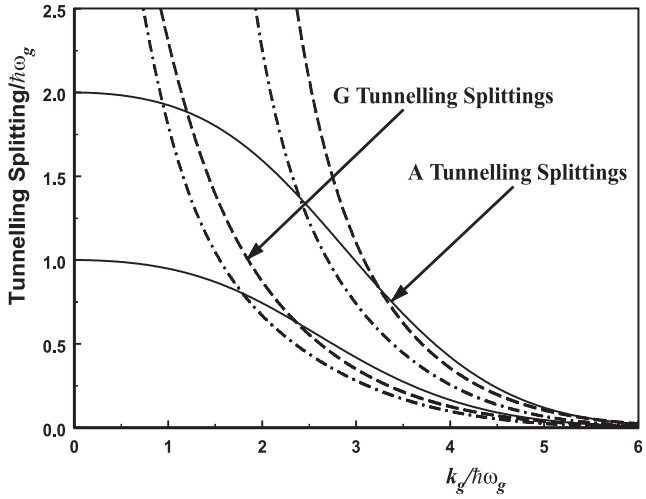

Figure 2. Comparison of the scale transformation (dashed), perturbation-corrected (dot–dashed) and isotropic (solid) tunnelling splittings between the A and G tunnelling states and the ground H tunnelling state for the pure $H \otimes g$ JT problem, as a function of $k_g/\hbar\omega_g$.

the symmetry is reduced to D_{5d}. Thus the correct form for Λ_{h_b} involves $\{\lambda_a, \lambda_{e_1}, \lambda_{e_1}, \lambda_{e_2}, \lambda_{e_2}\}$. The S-matrices that reduce the symmetry to these local modes are given in the appendix.

Following the same procedure as for the D_{3d} wells, we find that the energy of any D_{5d} minimum corrected to second order in perturbation theory is

$$\mathcal{H}_{AA}^{D_{5d}} = \frac{\hbar\omega_h}{2}\left[-\frac{4}{5}k_{h_b}'^2 + \frac{\lambda_a}{2} + \frac{1}{2\lambda_a} + \lambda_{e_1} + \frac{1}{\lambda_{e_1}} + \lambda_{e_2} + \frac{1}{\lambda_{e_2}} - \frac{k_{h_b}'^2}{10(1+k_{h_b}'^2)}\left(\frac{1}{\lambda_{e_1}} + \frac{1}{\lambda_{e_2}}\right)\right] \tag{40}$$

where $k'_{h_b} = k_{h_b}/\hbar\omega_h$. If the $\lambda_{\Gamma'}$ in this expression are replaced by unity, the isotropic energy given in [17] is regained, plus a second-order correction. This second-order correction is responsible for lifting the degeneracy of the vibronic mode. Minimization of the energy with respect to the $\lambda_{\Gamma'}$ results in

$$\begin{aligned} \lambda_a &= 1 \\ \lambda_{e1} = \lambda_{e2} &= \sqrt{1 - \frac{k_{h_b}'^2}{10k_{h_b}'^2 + 10}}. \end{aligned} \tag{41}$$

Thus the frequency of the a mode is unaffected by anisotropy but the e_1 and e_2 modes behave identically. The two e modes are accidentally degenerate through underlying deeper symmetry within the D_{5d} minima. The frequency of the e modes is reduced by a factor of $\sqrt{9/10} \approx 0.95$ in the infinite-coupling limit. As this is very close to one, anisotropic effects have very little effect on the D_{5d} minima. It should be noted that $\mathcal{H}_{AA}^{D_{5d}}$ with the above frequencies gives correct tunnelling energies in the infinite-coupling limit. Thus the theory derived above is an improvement over that presented originally in Dunn and Bates [19].

In order to calculate the energies of the H and A tunnelling states using the expressions

$$\begin{aligned} E_A^{D_{5d}} &= \frac{\mathcal{H}_{AA}^{D_{5d}} + 5\mathcal{H}_{AB}^{D_{5d}}}{1 + 5S_{AB}^{D_{5d}}} \\ E_H^{D_{5d}} &= \frac{\mathcal{H}_{AA}^{D_{5d}} - \mathcal{H}_{AB}^{D_{5d}}}{1 - S_{AB}^{D_{5d}}} \end{aligned} \tag{42}$$

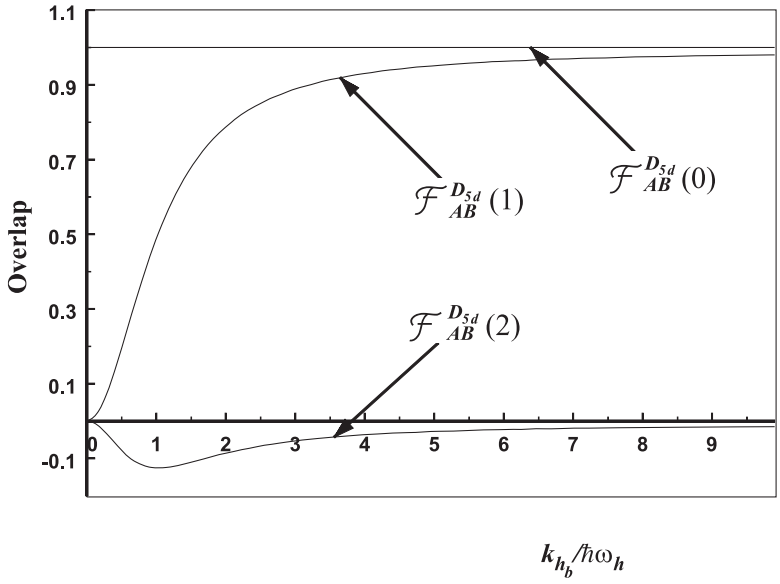

Figure 3. Zeroth-, first- and second-order contributions to the anisotropic overlap between wells A and B for the D_{5d} minima, as a function of $k_{h_b}/\hbar\omega_h$ (with each term divided by the zeroth-order overlap).

derived previously [15–17], the anisotropic overlaps and matrix elements between the two wells A and B, for example, must first be found using the general expressions derived above. The overlap is given by equation (22). The zeroth-order overlap is

$$S_{AB}^{(0)} = -\sqrt{\frac{12k_{h_b}'^2\lambda_{e1}}{5(3\lambda_{e1}+2)(2\lambda_{e1}+3)}}\exp\left(\frac{-\lambda_{e1}}{(3\lambda_{e1}+2)}\right) \tag{43}$$

and the perturbation corrections are given by

$$\mathcal{F}_{AB}^{(1)} = \frac{24}{5}\frac{k_{h_b}'^2}{(k_{h_b}'^2+1)(3\lambda_{e1}+2)}$$

$$\mathcal{F}_{AB}^{(2)} = -\frac{3}{100}\frac{k_{h_b}'^2(5(3\lambda_{e1}+2)(19{\lambda_{e1}}^2+42\lambda_{e1}+19)+8k_{h_b}'^2\lambda_{e1}(3+2\lambda_{e1}))}{\lambda_{e1}(k_{h_b}'^2+1)^2(3\lambda_{e1}+2)^2(3+2\lambda_{e1})}. \tag{44}$$

Figure 3 shows a plot of the zeroth-, first- and second-order overlaps, with the zeroth-order overlap factorized out. It can be seen that, in the strong-coupling regime, the first-order overlap is not negligible but instead approaches the zeroth-order term. This result obviously throws doubt on the way the Hamiltonian was initially separated into the two parts $\tilde{\mathcal{H}}_1'$ and $\tilde{\mathcal{H}}_2'$. However, it was shown in section 3 that the coefficients of the first-and second-order terms in the wavefunction approach zero at high coupling, which would appear to contradict this result. The explanation for this apparent discrepancy lies in the fact that the excited phonon states are more spread out. At strong coupling, the wavefunction is dominated by the zero-phonon state with only a very small contribution from the one-phonon states. However, because the one-phonon state is much more spread out than the zero-phonon state, the overlap between a zero-phonon and a one-phonon state is substantially greater than a zero-phonon to zero-phonon overlap. Therefore, the perturbation theory is not valid for the overlap, but it is valid for the wavefunction itself. At the end of this section, it will be seen that the perturbation correction

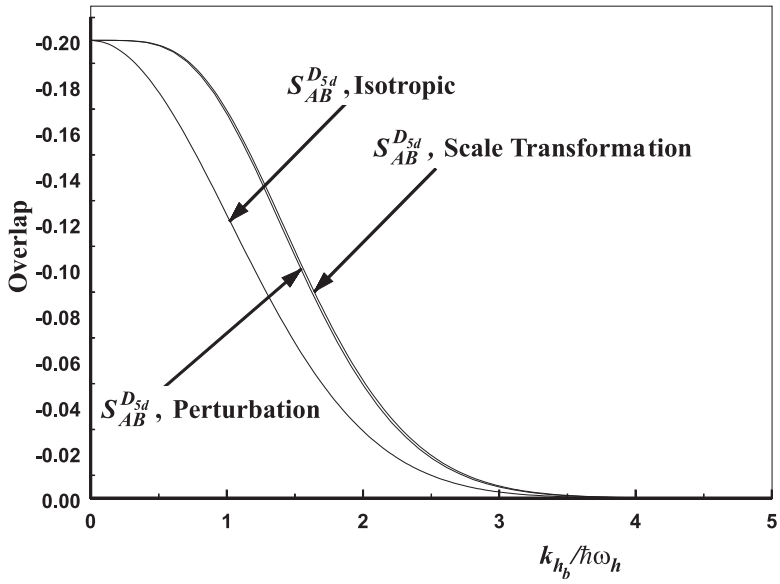

Figure 4. Anisotropic and isotropic overlaps between wells A and B as a function of $k_{h_b}/\hbar\omega_h$ for the D_{5d} minima.

to the tunnelling energies is very small, so that the method remains valid for regions which apply to realistic experimental situations.

Figure 4 shows a plot of the anisotropic overlap, with the isotropic overlap shown for comparison. Also shown in the figure is the perturbation-corrected overlap without the scale transformation. This graph shows that, on including the perturbation corrections, the overlap between the two minima increases considerably for reasons discussed above. The scale transformation has less effect, but also increases the overlap. This increase occurs because the scale transformation replaces the original degenerate frequency by the local mode frequency, which is always less than the original frequency. The phonon states are therefore even more spread out, leading to the observed increase in overlap.

The matrix element of the Hamiltonian within a well has been calculated above. The matrix element between wells A and B is much more complicated to evaluate. From equation (28), the zeroth-order matrix element of the oscillator Hamiltonian is

$$(\mathcal{H}_{\rm osc})_{AB}^{(0)} = S_{AB}^{(0)}\left(\frac{9\lambda_{e_1}^4 + 32\lambda_{e_1}^3 + 43\lambda_{e_1}^2 + 32\lambda_{e_1} + 9}{2\lambda_{e_1}(3\lambda_{e_1}+2)(2\lambda_{e_1}+3)} - 2k_{h_b}'^2\frac{3\lambda_{e_1}^2 - 2}{(3\lambda_{e_1}+2)^2}\right)\hbar\omega_h \tag{45}$$

and the perturbation corrections are

$$\mathcal{G}_{AB}^{(1)} = -12\frac{(1+\lambda_{e1})k_{h_b}'^2}{(k_{h_b}'^2+1)(3\lambda_{e1}+2)^2},$$

$$\mathcal{G}_{AB}^{(2)} = \frac{1}{20}\frac{k_{h_b}'^2}{\lambda_{e1}^2(k_{h_b}'^2+1)^2(3\lambda_{e1}+2)^3(3+2\lambda_{e1})^2}(5(3\lambda_{e1}+2)(27{\lambda_{e1}}^6 + 117{\lambda_{e1}}^5 + 211{\lambda_{e1}}^4 + 240{\lambda_{e1}}^3 + 211{\lambda_{e1}}^2 + 117\lambda_{e1} + 27) + 24k_{h_b}'^2{\lambda_{e1}}^2(1+\lambda_{e1})(3+2\lambda_{e1})^2). \tag{46}$$

The first-order perturbation correction approaches the zeroth-order term in strong coupling for the same reason as that occurring in the overlap terms.

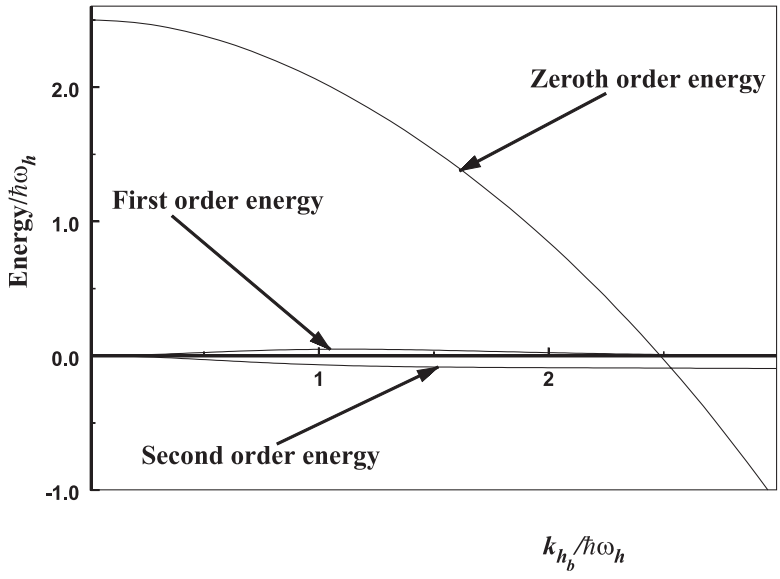

Figure 5. Zeroth-, first- and second-order contributions to the anisotropic tunnelling energies of the H State for the D_{5d} Minima, as a function of $k_{h_b}/\hbar\omega_h$.

The zeroth-, first- and second-order contributions to the matrix element of the interaction Hamiltonian are given by

$$(\mathcal{H}_{\rm int})^{(0)}_{AB} = -\frac{4k'^2_{h_b}\hbar\omega_h S^{(0)}_{AB}}{3\lambda_{e1}+2}$$

$$(\mathcal{H}_{\rm int})^{(1)}_{AB} = -\frac{k'^2_{h_b}\hbar\omega_h S^{(0)}_{AB}[5(3\lambda_{e1}+2)(15\lambda^2_{e1}+4\lambda_{e1}-9)+(144\lambda^2_{e1}+216\lambda_{e1})k'^2_{h_b}]}{10(k'^2_{h_b}+1)(3+2\lambda_{e1})(3\lambda_{e1}+2)^2\lambda_{e1}}$$

$$(\mathcal{H}_{\rm int})^{(2)}_{AB} = -\frac{k'^4_{h_b}\hbar\omega_h S^{(0)}_{AB}[5(3\lambda_{e1}+2)(57{\lambda_{e1}}^2+122\lambda_{e1}+51)+24k'^2_{h_b}\lambda_{e1}(3+2\lambda_{e1})]}{100(3\lambda_{e1}+2)^3(3+2\lambda_{e1})(k'^2_{h_b}+1)^2\lambda_{e1}}. \quad (47)$$

It is found that the effect of anisotropy is to increase the size of the overall matrix element in a similar way to that which occurred in the calculation of the overlap.

The calculated zeroth-, first- and second-order contributions to the energies of the H state are shown in figure 5. It is quite clear that the first- and second-order contributions are small compared to the zeroth-order terms, which is not surprising as anisotropic changes in the frequencies are small. Results for the A state are similar, except that the first- and second-order corrections are slightly larger in weak coupling. Nevertheless, they are at most 15% of the zeroth-order value. However, there is clearly a problem with the perturbation corrections to the A state in the weak-coupling limit. This arises because, in the expression for the energy of the A state, both the numerator and denominator tend to zero in the weak-coupling limit although there is a well defined limit in the isotropic case. However, perturbation theory in this limit is no longer always well defined. This arises as the perturbation approach is valid only in strong coupling when the energy levels are far apart. An alternative explanation is that the off-diagonal matrix element $H^{D_{5d}}_{AB}$ contains some third-order terms. This arises because, when the expression for this matrix element is evaluated, it is impossible to separate the Hamiltonian, as different unitary transformations appear on each side of it. In both the numerator and denominator the expression for the energy of the A state becomes zero in the weak-coupling

limit so that these third-order terms could have a large effect. The tunnelling splitting between the H and A vibronic states was illustrated in figure 1 in [16] as a function of k_{h_b}. This figure showed that the calculated splitting including the anisotropic contributions agreed well with results of numerical diagonalization in the strong-coupling regime.

5. Conclusions

This paper has developed a new analytical model of anisotropy, and shown how the results can be applied to the $H \otimes (h \oplus g)$ JT system. The tunnelling states obtained have the correct anisotropic energy in the limit of strong vibronic coupling, unlike analytical results obtained when anisotropy is neglected [19]. Although the new model results in complicated algebraic expressions for the overlaps and matrix elements, especially when there are D_{3d} minima in the APES, the expressions obtained are readily computable. Even though the results are complicated, there are still advantages in having algebraic expressions over the alternative of numerical results. For example, the form of the states more clearly illustrates the underlying physics. The results are also more readily used for further calculations where the energy levels are needed, such as the determination of vibronic (Ham) reduction factors. Furthermore, it should be noted that the $H \otimes (h \oplus g)$ JT system contains the highest possible vibronic and electronic degeneracies, so results for any other cubic or icosahedral system will be rather less complicated.

Acknowledgment

One of us (YML) wishes to thank the University of Nottingham for a Research Fellowship.

Appendix

In this appendix, the various S-matrices needed for the scale transformation calculation are given. These matrices were found by calculating the curvature matrix of the energy surface at the point of the minimum in question, using the method of Öpik and Pryce [20].

For the D_{5d} minima, only two matrices are needed, namely

$$S_A^{D_{5d}} = \sqrt{\tfrac{1}{10}} \begin{pmatrix} \sqrt{3} & 1 & \sqrt{6} & 0 & 0 \\ 0 & 0 & 0 & 0 & \sqrt{10} \\ 0 & 0 & 0 & \sqrt{10} & 0 \\ -\sqrt{20/3} & 0 & \sqrt{10/3} & 0 & 0 \\ -\sqrt{1/3} & 3 & -\sqrt{2/3} & 0 & 0 \end{pmatrix}$$

$$S_B^{D_{5d}} = \sqrt{\tfrac{1}{10}} \begin{pmatrix} \sqrt{3} & 1 & -\sqrt{6} & 0 & 0 \\ 0 & 0 & 0 & 0 & \sqrt{10} \\ 0 & 0 & 0 & \sqrt{10} & 0 \\ \sqrt{20/3} & 0 & \sqrt{10/3} & 0 & 0 \\ -\sqrt{1/3} & 3 & \sqrt{2/3} & 0 & 0 \end{pmatrix}. \tag{A.1}$$

For the D_{3d} minima six matrices are needed, three for the h vibrational mode and three

for the g vibrational mode. The h matrices are

$$S^{D_{3d}}_{h,a} = \begin{pmatrix} 0 & 0 & \frac{1}{3}\sqrt{3} & \frac{1}{3}\sqrt{3} & \frac{1}{3}\sqrt{3} \\ -\frac{1}{4}\sqrt{12} & 0 & -\frac{1}{12}\sqrt{6} & -\frac{1}{12}\sqrt{6} & \frac{1}{6}\sqrt{6} \\ 0 & \frac{1}{2}\sqrt{3} & -\frac{1}{4}\sqrt{2} & \frac{1}{4}\sqrt{2} & 0 \\ 0 & \frac{1}{2} & \frac{1}{4}\sqrt{6} & -\frac{1}{4}\sqrt{6} & 0 \\ \frac{1}{2} & 0 & -\frac{1}{4}\sqrt{2} & -\frac{1}{4}\sqrt{2} & \frac{1}{2}\sqrt{2} \end{pmatrix}$$

$$S^{D_{3d}}_{h,b} = \begin{pmatrix} 0 & 0 & -\frac{1}{3}\sqrt{3} & \frac{1}{3}\sqrt{3} & \frac{1}{3}\sqrt{3} \\ 0 & \frac{1}{2}\sqrt{3} & -\frac{1}{4}\sqrt{2} & -\frac{1}{4}\sqrt{2} & 0 \\ \frac{1}{4}\sqrt{12} & 0 & \frac{1}{12}\sqrt{6} & -\frac{1}{12}\sqrt{6} & \frac{1}{6}\sqrt{6} \\ -\frac{1}{2} & 0 & \frac{1}{4}\sqrt{2} & -\frac{1}{4}\sqrt{2} & \frac{1}{2}\sqrt{2} \\ 0 & \frac{1}{2} & \frac{1}{4}\sqrt{6} & \frac{1}{4}\sqrt{6} & 0 \end{pmatrix} \tag{A.2}$$

$$S^{D_{3d}}_{h,e} = \begin{pmatrix} -\frac{1}{6}\sqrt{6} & \frac{1}{2}\sqrt{2} & -\frac{1}{3}\sqrt{3} & 0 & 0 \\ -\frac{1}{6}\sqrt{3} & \frac{1}{2} & \frac{1}{3}\sqrt{6} & 0 & 0 \\ 0 & 0 & 0 & \frac{1}{2}\sqrt{2} & \frac{1}{2}\sqrt{2} \\ \frac{1}{2}\sqrt{3} & \frac{1}{2} & 0 & 0 & 0 \\ 0 & 0 & 0 & \frac{1}{2}\sqrt{2} & -\frac{1}{2}\sqrt{2} \end{pmatrix}.$$

The g mode matrices are

$$S^{D_{3d}}_{g,a} = \begin{pmatrix} 0 & \frac{1}{3}\sqrt{3} & \frac{1}{3}\sqrt{3} & \frac{1}{3}\sqrt{3} \\ 1 & 0 & 0 & 0 \\ 0 & -\frac{1}{2}\sqrt{2} & 0 & \frac{1}{2}\sqrt{2} \\ 0 & -\frac{1}{6}\sqrt{6} & \frac{1}{3}\sqrt{6} & -\frac{1}{6}\sqrt{6} \end{pmatrix}$$

$$S^{D_{3d}}_{g,b} = \begin{pmatrix} 1 & 0 & 0 & 0 \\ 0 & \frac{1}{3}\sqrt{3} & -\frac{1}{3}\sqrt{3} & -\frac{1}{3}\sqrt{3} \\ 0 & 0 & \frac{1}{2}\sqrt{2} & -\frac{1}{2}\sqrt{2} \\ 0 & \frac{1}{3}\sqrt{6} & \frac{1}{6}\sqrt{6} & \frac{1}{6}\sqrt{6} \end{pmatrix} \tag{A.3}$$

$$S^{D_{3d}}_{g,e} = \begin{pmatrix} 0 & 0 & -\frac{1}{2}\sqrt{2} & \frac{1}{2}\sqrt{2} \\ -\frac{1}{6}\sqrt{6} & \frac{1}{6}\sqrt{30} & 0 & 0 \\ \frac{1}{6}\sqrt{30} & \frac{1}{6}\sqrt{6} & 0 & 0 \\ 0 & 0 & \frac{1}{2}\sqrt{2} & \frac{1}{2}\sqrt{2} \end{pmatrix}.$$

References

[1] Liu Y M, Bates C A, Dunn J L and Polinger V Z 1996 *J. Phys.: Condens. Matter* **8** L523
[2] Dunn J L and Eccles M R 2001 *Phys. Rev.* B **64** 195104
[3] Liu Y M, Dunn J L, Bates C A and Polinger V Z 1997 *Z. Phys. Chem.* **200** 111
[4] Liu Y M, Dunn J L, Bates C A and Polinger V Z 1997 *J. Phys.: Condens. Matter* **9** 7119
[5] Qiu Q C, Dunn J L, Bates C A and Liu Y M 1998 *Phys. Rev.* B **58** 4406

[6] Moate C P, Liu Y M, Dunn J L and Bates C A 1999 *Electron–Phonon Dynamics and Jahn–Teller Effect* (Singapore: World Scientific) p 258
[7] Canton S E, Yencha A J, Kukk E, Bozek J D, Lopes M C A, Snell G and Berrah N 2002 *Phys. Rev. Lett.* **89** 045502
[8] Fowler P W and Ceulemans A 1985 *Mol. Phys.* **54** 767
[9] Ceulemans A and Fowler P W 1990 *J. Chem. Phys.* **93** 1221
[10] Cullerne J P, Angelova M N and O'Brien M C M 1995 *J. Phys.: Condens. Matter* **7** 3247
[11] De Los Rios P, Manini N and Tosatti E 1996 *Phys. Rev.* B **54** 7157
[12] Manini N and De Los Rios P 2000 *Phys. Rev.* B **62** 29
[13] Koç R, Tütüncüler H and Koca M 2000 *Eur. Phys. J.* D **12** 467
[14] Manini N, Dal Corso A, Fabrizio M and Tosatti E 2001 *Phil. Mag.* B **81** 793
[15] Moate C P, O'Brien M C M, Dunn J L, Bates C A, Liu Y M and Polinger V Z 1996 *Phys. Rev. Lett.* **77** 4362
[16] Moate C P, Dunn J L, Bates C A and Liu Y M 1997 *Z. Phys. Chem.* **200** 137
[17] Moate C P, Dunn J L, Bates C A and Liu Y M 1997 *J. Phys.: Condens. Matter* **9** 6049
[18] Polinger V Z, Huang R, Dunn J L and Bates C A 2002 *J. Chem. Phys.* **117** 4340
[19] Dunn J L and Bates C A 1989 *J. Phys.: Condens. Matter* **1** 375
[20] Öpik U and Pryce M H L 1957 *Proc. R. Soc.* A **238** 425
[21] Joshi A W 1984 *Matrices and Tensors in Physics* (New Delhi: Wiley)
[22] Dunn J L 1988 *J. Phys. C: Solid State Phys.* **21** 383